Received: 12 February 2018 | Revised: 1 April 2019 | Accepted: 10 April 2019

DOI: 10.1111/geb.12937

RESEARCH PAPER

Global Ecology and Biogeography A Journal of Macroecology WILEY

Covariations between plant functional traits emerge from constraining parameterization of a terrestrial biosphere model

Marc Peaucelle[1,2] | Cédric Bacour[3] | Philippe Ciais[1] | Nicolas Vuichard[1] | Sylvain Kuppel[4] | Josep Peñuelas[2,5] | Luca Belelli Marchesini[6,7] | Peter D. Blanken[8] | Nina Buchmann[9] | Jiquan Chen[10] | Nicolas Delpierre[11] | Ankur R. Desai[12] | Eric Dufrene[11] | Damiano Gianelle[6] | Cristina Gimeno-Colera[13] | Carsten Gruening[14] | Carole Helfter[15] | Lukas Hörtnagl[9] | Andreas Ibrom[16] | Richard Joffre[17] | Tomomichi Kato[18,19] | Thomas E. Kolb[20] | Beverly Law[21] | Anders Lindroth[22] | Ivan Mammarella[23] | Lutz Merbold[24] | Stefano Minerbi[25] | Leonardo Montagnani[25,26] | Ladislav Šigut[27] | Mark Sutton[15] | Andrej Varlagin[28] | Timo Vesala[29,30] | Georg Wohlfahrt[31] | Sebastian Wolf[32] | Dan Yakir[33] | Nicolas Viovy[1]

[1]Laboratoire des Sciences du Climat et de l'Environnement, CEA/CNRS/UVSQ, Gif-sur-Yvette, France

[2]CREAF, Barcelona, Spain

[3]NOVELTIS, Labège, France

[4]Northern Rivers Institute, University of Aberdeen, Aberdeen, UK

[5]CSIC, Global Ecology Unit CREAF-CSIC-UAB, Barcelona, Spain

[6]Department of Sustainable Agro-Ecosystems and Bioresources, Research and Innovation Centre, Fondazione Edmund Mach, San Michele all'Adige, Italy

[7]Department of Landscape Design and Sustainable Ecosystems, Agrarian-Technological Institute, RUDN University, Moscow, Russia

[8]Department of Geography, University of Colorado, Boulder, Colorado

[9]Institute of Agricultural Sciences, ETH Zurich, Zurich, Switzerland

[10]LEES Lab, Department of Geography and Spatial Sciences, Michigan State University, East Lansing, Michigan

[11]Ecologie Systématique Evolution, Univ. Paris-Sud, CNRS, AgroParisTech, Université Paris-Saclay, Orsay, France

[12]Department of Atmospheric and Oceanic Sciences, University of Wisconsin–Madison, Madison, Wisconsin

[13]Fundación CEAM, Parque Tecnológico, Paterna, Spain

[14]European Commission, Joint Research Centre, Ispra, Italy

[15]Centre for Ecology and Hydrology, Penicuik, UK

[16]Department of Environmental Engineering, Technical University of Denmark, Lyngby, Denmark

[17]CEFE, CNRS – Université de Montpellier – Université Paul-Valéry Montpellier – EPHE – IRD, Montpellier, France

[18]Research Faculty of Agriculture, Hokkaido University, Sapporo, Japan

[19]Global Station for Food, Land and Water Resources (GSF), GI-CoRE, Hokkaido University, Sapporo, Japan

[20]School of Forestry, Northern Arizona University, Flagstaff, Arizona

[21]Forest Ecosystems and Society Dept, College of Forestry, Oregon State University, Corvallis, Oregon

[22]Department of Physical Geography and Ecosystem Science, Lund University, Lund, Sweden

[23]Institute for Atmosphere and Earth System Research/Physics, Faculty of Science, University of Helsinki, Helsinki, Finland

[24]Mazingira Centre, International Livestock Research Institute (ILRI), Nairobi, Kenya

[25]Forest Services, Autonomous Province of Bolzano, Bolzano, Italy

[26]Faculty of Science and Technology, Free University of Bolzano, Piazza Università, Bolzano, Italy

[27]Department of Matter and Energy Fluxes, Global Change Research Institute CAS, Brno, Czech Republic

[28]A.N. Severtsov Institute of Ecology and Evolution, Russian Academy of Sciences, Moscow, Russia
[29]Institute for Atmosphere and Earth System Research/Forest Sciences, Faculty of Agriculture and Forestry, University of Helsinki, Helsinki, Finland
[30]Viikki Plant Science, University of Helsinki, Helsinki, Finland
[31]Institute for Ecology, University of Innsbruck, Innsbruck, Austria
[32]Institute of Terrestrial Ecosystems, ETH Zurich, Zurich, Switzerland
[33]Earth and Planetary Sciences, Weizmann Institute of Science, Rehovot, Israel

Correspondence
Marc Peaucelle, Laboratoire des Sciences du Climat et de l'Environnement, CEA/CNRS/UVSQ, Gif-sur-Yvette, France.
Email: marc.peaucelle@lsce.ipsl.fr

Funding information
European Research Council, Grant/Award Number: Synergy grant ERC-SyG-2013-610028 IMBALANCE-P

Editor: Jonathan Lenoir

Abstract

Aim: The mechanisms of plant trait adaptation and acclimation are still poorly understood and, consequently, lack a consistent representation in terrestrial biosphere models (TBMs). Despite the increasing availability of geo-referenced trait observations, current databases are still insufficient to cover all vegetation types and environmental conditions. In parallel, the growing number of continuous eddy-covariance observations of energy and CO_2 fluxes has enabled modellers to optimize TBMs with these data. Past attempts to optimize TBM parameters mostly focused on model performance, overlooking the ecological properties of ecosystems. The aim of this study was to assess the ecological consistency of optimized trait-related parameters while improving the model performances for gross primary productivity (GPP) at sites.

Location: Worldwide.

Time period: 1992–2012.

Major taxa studied: Trees and C_3 grasses.

Methods: We optimized parameters of the ORCHIDEE model against 371 site-years of GPP estimates from the FLUXNET network, and we looked at global covariation among parameters and with climate.

Results: The optimized parameter values were shown to be consistent with leaf-scale traits, in particular, with well-known trade-offs observed at the leaf level, echoing the leaf economic spectrum theory. Results showed a marked sensitivity of trait-related parameters to local bioclimatic variables and reproduced the observed relationships between traits and climate.

Main conclusions: Our approach validates some biological processes implemented in the model and enables us to study ecological properties of vegetation at the canopy level, in addition to some traits that are difficult to observe experimentally. This study stresses the need for: (a) implementing explicit trade-offs and acclimation processes in TBMs; (b) improving the representation of processes to avoid model-specific parameterization; and (c) performing systematic measurements of traits at FLUXNET sites in order to gather information on plant ecophysiology and plant diversity, together with micro-meteorological conditions.

KEYWORDS
data assimilation, optimization, ORCHIDEE, plant acclimation, plant functional traits, terrestrial model

1 | INTRODUCTION

Terrestrial biosphere models (TBMs) describe the different processes controlling exchanges of energy and trace gases between the atmosphere and the biosphere. Process-based TBMs are useful tools for understanding the dynamics of ecosystems under changing environment, for present-day to future conditions.

In most TBMs, the worldwide vegetation is divided into plant functional types (PFTs) based on general characteristics of the photosynthetic pathways, phenology, structure and physiology. Different PFTs usually share the same equations but use different parameter values to describe generic processes (photosynthesis, respiration), whereas biome-specific equations may be used for phenology and allocation. Therefore, for a given PFT, only the differences in climate and soil properties can determine spatial and temporal gradients in ecosystem state variables.

The prescribed values of PFT-specific parameters are derived from discrete observations obtained at varying spatial scales (organs, individuals or ecosystems; Kattge, Knorr, Raddatz, & Wirth, 2009; Reich, Wright, & Lusk, 2007) and in specific environmental conditions, despite the modulation of real-world plant traits by climate (Maire et al., 2015; Ordoñez et al., 2009; van Ommen Kloeke, Douma, Ordonez, Reich, & Bodegom, 2012; Wright et al., 2005) and soil properties (Fisher, Badgley, & Blyth, 2012). In addition, some TBM parameters relate to traits that are difficult to measure experimentally (e.g., root turnovers or carbon allocation) or are model specific. These parameters can hardly be optimized directly from observations, and their adjustment to varying environmental conditions can be determined only by labour-intensive multifactorial ecosystem manipulation experiments (Luo, Jiang, Niu, & Zhou, 2017). This rigid determination of parameter values, combined with the use of single PFTs to cover a range of different species (Peaucelle, Bellassen, Ciais, Peñuelas, & Viovy, 2017), hinders a realistic representation of the past, present and future ecosystem dynamics, at both the local and the regional scale, and their response to global drivers, such as climate, elevated CO_2 and nutrient fertilization (Atkin et al., 2015; Hartig et al., 2012; Kroner & Way, 2016; Reich et al., 2016).

To overcome the rigidity of the PFT representation, various approaches have been proposed to provide continuous distributions of plant functional traits related to model parameters. These approaches range from extrapolating trait observations across spatial gradients (Verheijen et al., 2015) to estimating optimal trait values according to ecological theories and plant-centred approaches (Pavlick, Drewry, Bohn, Reu, & Kleidon, 2013; Prentice, Dong, Gleason, Maire, & Wright, 2014; Reu et al., 2011). The drawback of these different approaches is that they require both spatial and temporal observations for model calibration and/or validation. Despite the increasing number of geo-referenced trait observations (Kattge et al., 2011), current databases are insufficient to cover all vegetation types and environmental conditions for projections at the ecosystem level (Musavi et al., 2015, 2016). Moreover, trait observations should be co-located with process and meteorology data to understand linkages between traits and ecosystem function (Law et al., 2008), which is rare in existing databases, although increasingly being addressed for some biomes (Bjorkman et al., 2018). Long-term monitoring of functional traits is needed to assess the adjustments to climate. Given that such information is still lacking, approaches have been developed that confound the spatial and temporal dimensions of trait variability.

Another modelling strategy consists of optimizing TBMs against observed variables sensitive to ecosystem-level parameters in order to overcome these limitations. This approach assumes that the model structure is unbiased, so that realistic parameters values can be estimated when model simulations best match observations. Given that biometric variables are sparse and often depend on processes not represented in models (Thum et al., 2017), energy and trace gas flux measurements are more appealing to optimize TBM parameters.

Eddy-covariance data provide near-continuous observations of CO_2, latent heat and sensible heat fluxes, and are therefore well suited for better constraining photosynthesis, respiration, transpiration and carbon phenology model parameters. Eddy-covariance measurements have been used extensively to improve specific performances of TBMs (i.e., their ability to reproduce specific observed ecosystem behaviours; Carvalhais et al., 2010; Kuppel et al., 2012; Santaren, Peylin, Bacour, Ciais, & Longdoz, 2014; Schürmann et al., 2016). However, such model calibrations are disconnected, by construction, from ecological theory or trait-based relationships and do not exploit the full potential of continuous flux observations across the globe, which provide both spatial and temporal information.

In this study, we aim to assess the consistency of model trait parameters optimized against eddy-covariance flux tower measurements of growth primary productivity (GPP) using the state-of-the-art Organising Carbon and Hydrology In Dynamic Ecosystems (ORCHIDEE) land surface model (Krinner et al., 2005). In addition to classical optimization analyses (i.e., looking for the optimal parameter sets that result in the greatest model improvement), we focus here on the variability of optimized parameter values and on inter-traits correlations or trait–environment correlations. By doing so, we address the following research questions: (a) are the parameters retrieved by optimizing the model against flux tower records consistent with known relationships between traits (i.e., trade-offs), or (b) between traits and environmental variables? (c) What new relationship can be identified with this approach?

2 | METHODS

2.1 | The ORCHIDEE model

The land surface model ORCHIDEE (v.1.9.6, without nitrogen cycle) computes biosphere–atmosphere exchanges, consistently with water and carbon storage, using ordinary differential equations (Krinner et al., 2005) (Figure1). Given meteorological forcing, plant and soil conditions, the model simulates photosynthesis, all components of the surface energy budget and hydrological processes with a half-hourly time step, whereas the dynamics of carbon storage are calculated daily. In ORCHIDEE, the land surface is discretized into 12 PFTs and bare soil (Supporting Information Appendix S1, Table

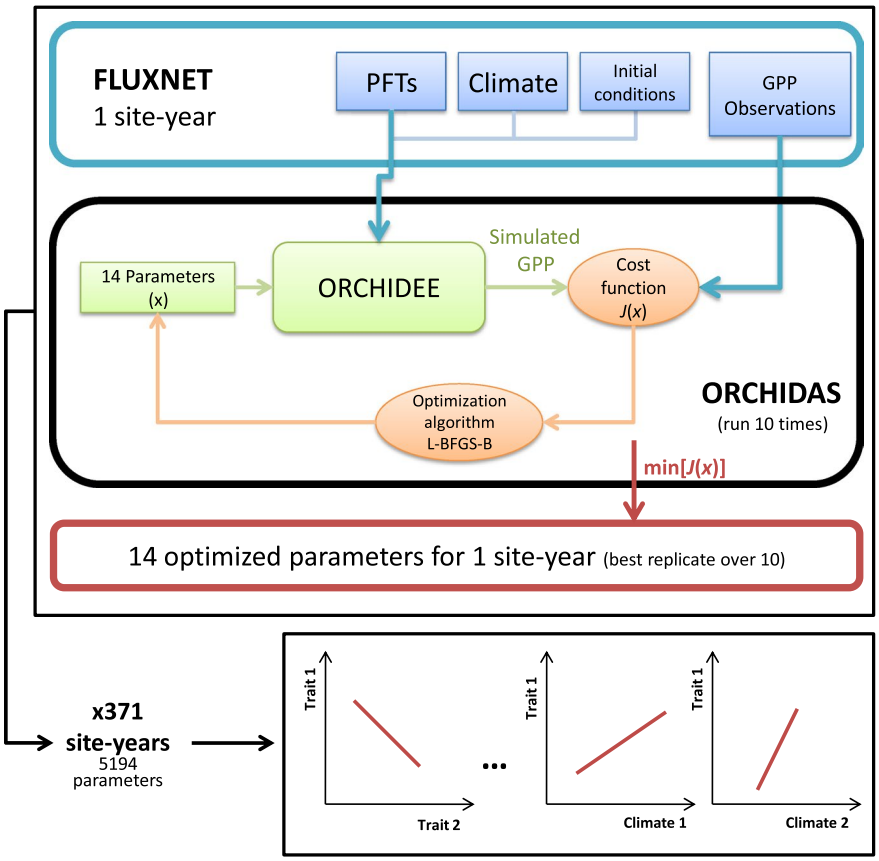

FIGURE 1 Schematic representation of the modelling protocol followed in this study. For each FLUXNET site-year (blue), the model ORCHIDEE (green) was calibrated with the data assimilation system ORCHIDAS (red) in order to reproduce gross primary productivity (GPP) observations. The ORCHIDAS system uses a gradient-based approach (L-BFGS-B) to reduce the cost function $J(x)$. For each site-year, 14 parameters (listed in Table 1) were optimized 10 times with different initial values. The best calibration [i.e., leading to the minimum value of $J(x)$] was retained. This procedure was repeated for each site-year, resulting in 371 sets of 14 independently optimized parameters. Finally, correlations between optimized parameters and climate were explored using standardized major axis regressions [Colour figure can be viewed at wileyonlinelibrary.com]

S1.1). All PFTs share the same equations but use different parameter values, except for phenology (budburst/senescence), which is PFT specific (Botta, Viovy, Ciais, Friedlingstein, & Monfray, 2000).

2.2 | Eddy-covariance gross primary productivity

We used half-hourly flux observations from eddy-covariance sites within the FLUXNET network (https://fluxnet.fluxdata.org). The sites were selected on the basis of spatial homogeneity and the dominance of a vegetation type that could be matched easily to one of the PFTs in ORCHIDEE, excluding crops and C_4 grasses. The vegetation type information at each site was obtained from http://fluxnet.ornl.gov. A list of analysed FLUXNET sites (98 sites, 371 site-years) and the corresponding PFTs is given in the Supporting Information (Appendix S2). The following analyses rely on GPP derived from net ecosystem exchange (NEE; reference with variable USTAR - friction velocity threshold) after accounting for ecosystem respiration calculated using the method of Reichstein et al., (2005) provided in the FLUXNET dataset. Years with <80% of available half-hourly observations were discarded.

2.3 | Meteorological data

Given that ORCHIDEE needs continuous half-hourly meteorological forcing, we filled the gaps in time series of weather variables using the interpolation algorithm developed by Vuichard and Papale (2015). Linear interpolation was applied between available observations when the gap duration in the meteorological data was <6 h. Otherwise, the variables were interpolated and bias corrected using the ERA-interim re-analysis (*c.* 80 km; Dee et al., 2011). Snow and rain were identified according to air temperature (threshold for snow being 0°C).

2.4 | Data assimilation procedure

The parameters of ORCHIDEE were optimized with the ORCHIDAS package developed by Kuppel et al. (2012), Bacour et al. (2015), MacBean et al. (2015) and Peylin et al. (2016) (https://orchidas.lsce.ipsl.fr/; Figure 1). Gaussian distributions of parameter and observation errors were assumed, and a gradient-based approach was used to minimize the Bayesian cost function, J (Tarantola, 2005):

$$J(x)=\frac{1}{2}\left[(\mathbf{y}-H(x))^{\mathrm{T}}\mathbf{R}^{-1}(\mathbf{y}-H(x))+(\mathbf{x}-\mathbf{x_b})^{\mathrm{T}}\mathbf{B}^{-1}(\mathbf{x}-\mathbf{x_b})\right] \quad (1)$$

This function quantifies the difference between observations ($\mathbf{y}$) and simulations [$H(x)$; here, GPP), and between a priori ($\mathbf{x_b}$) and optimized parameters ($\mathbf{x}$). The $\mathbf{B}$ and $\mathbf{R}$ matrices are the prior error covariance matrices for parameters and observations, respectively (including, in the latter case, eddy-covariance measurement and model errors).

Both $\mathbf{R}$ and $\mathbf{B}$ were taken as diagonal, as discussed by Kuppel et al. (2012). The $J(x)$ function was minimized iteratively with the L-BFGS-B algorithm (Byrd, Lu, Nocedal, & Zhu, 1995), which notably allows bounding the range of variation of the parameters to

TABLE 1 Description of the 14 optimized parameters and associated processes

Parameter	Description (units)	Processes involved
SLA	Specific leaf area (in square metres per gram of carbon)	Photosynthesis, phenology, allocation
Lage	Leaf lifespan (in days)	Photosynthesis, Phenology
Vcmax	Maximal carboxylation rate limited by CO_2 (in micromoles per square metre per second)	Photosynthesis
Vj/Vc	Ratio between the maximal carboxylation rate limited by light and *Vcmax*	Photosynthesis
Topt	Optimal temperature of the photosynthesis (in degrees Celsius)	Photosynthesis
gslope	Slope of the Ball–Berry relationship for the stomatal conductance	Photosynthesis, energy budget
LAImax	Maximal leaf area index	Photosynthesis, phenology, allocation
Klai	Minimal fraction of *LAImax* for the use of carbohydrate reserves	Allocation
bbdate	Budburst date (day of the year)	Phenology
tauleaf	Period after budburst during which the use of carbohydrates is allowed	Allocation
Csenes	Temperature for leaf senescence (used only for deciduous)	Phenology
Kbm	Multiplicative factor for the initial leaf biomass (used only for evergreens)	Phenology, allocation
Kroot	Exponential factor describing the root profile and depth	Water budget, photosynthesis
Wlim	Minimal threshold at which the photosynthesis becomes limited by water availability	Photosynthesis

Note: All the parameters are common to each plant functional type. *Kbm* and *bbdate* are scaling factors added to the model to improve the optimization of the seasonal cycle of the gross primary productivity but are not analysed in the study (for the detailed equations involving each parameter, see the Supporting Information (Appendix S1, Table S1.2).

optimize. After model calibration (i.e., minimizing *J*), the posterior error covariance matrix (***A***), providing the full statistical distribution of the optimized parameters was estimated by:

$$\boldsymbol{A}=\left[\boldsymbol{H}^{T}\boldsymbol{R}^{-1}\boldsymbol{H}+\boldsymbol{B}^{-1}\right]^{-1} \quad (2)$$

where ***H*** is the Jacobian of the model at the minimum of *J* (Tarantola, 2005). The covariances of errors between parameters contained in the non-diagonal terms of ***A*** inform about the ability of observations given the structure of ***H*** to solve for parameters individually or in combination. High error covariance between two parameters relates to the equifinality problem, whereby different values of these parameters result in model outputs equally matching the observations (relative to ***R***).

2.5 | Optimized parameters

We restricted our exercise to the parameters involved in the assimilation of CO_2, following previous sensitivity analyses from Kuppel (2012). We analysed 14 parameters controlling long-term and inter-annual GPP variability (Table 1). The key equations involving each optimized parameter and their effect on the simulated GPP are described in the Supporting Information (Appendix S1, Table S1.2). The parameters were related to photosynthetic capacity, phenology, carbon allocation and the water budget. Photosynthetic capacity parameters were the maximal rate of carboxylation limited by CO_2 (*Vcmax*), the ratio between the maximal rate of carboxylation limited by light and *Vcmax* (*Vj/Vc*), the optimal temperature of photosynthesis (*Topt*) and the slope of the Ball–Berry model for stomatal conductance (*gslope*). Parameters driving phenology were the specific leaf area (*SLA*), leaf longevity (*Lage*), summer maximal leaf area index (*LAImax*) and the temperature for leaf senescence (*Csenes*). Allocation parameters were the minimal fraction of *LAImax* for the use of carbohydrate reserves (*Klai*) and the period after budburst during which the use of carbohydrates is allowed (*tauleaf*) for the formation of new leaves. Finally, two parameters involved in the water status of the plant were the exponential factor describing the root profile and length (*Kroot*) and the minimal threshold at which photosynthesis becomes limited by minimum water potential (*Wlim*). In addition, two scaling factors, *Kbm* (initial biomass of leaves

for evergreen species) and *bbdate* (spring burdburst date), were added in the optimization to allow adjustment of the seasonal timing of GPP.

The range in variation of the three parameters corresponding to observable traits (*SLA*, *Vcmax* and *Lage*) was set from the TRY database for each PFT (Azevedo & Marenco, 2012; Cernusak, Hutley, Beringer, Holtum, & Turner, 2011; Deng et al., 2004; Domingues et al., 2010; Kattge et al., 2009, 2011; Meir, Levy, Grace, & Jarvis, 2007; Nascimento & Marenco, 2013; Niinemets, Oja, & Kull, 1999; van de Weg, Meir, Grace, & Ramos, 2012). Species from the TRY database were assigned to corresponding PFTs based on available metadata about plant structure, leaf phenology and climate information extracted from species' latitude and longitude coordinates. We chose as a reference range the 2.5th–97.5th percentile of the trait distributions from TRY. The variation ranges for the other parameters were fixed based on expert judgement (Kuppel et al., 2014).

2.6 | Simulations and assimilation set-up

At each flux tower site, we assumed that the eddy-covariance flux footprint was entirely composed by a single PFT (Supporting Information Appendix S2). The model was forced by local meteorological observations (see Section 2.3) and soil texture from the harmonized worldwide soil database (Nachtergaele et al., 2012) to define the residual and saturation water contents, and the saturated hydraulic conductivity in the soil model (Ducoudré, Laval, & Perrier, 1993; Krinner et al., 2005) based on Van Genuchten (1980). Initial soil carbon pools in equilibrium with local climate were obtained with an analytical spin-up procedure (Lardy, Bellocchi, & Soussana, 2011; Xia, Luo, Wang, Weng, & Hararuk, 2012). Initial biomass was simulated until reaching equilibrium (generally after *ac*. 300-year-long simulation using the studied year meteorological data and constant CO_2 set to the level of the year), thus different from the real stand age observed at each site.

We optimized GPP averaged over 15 days using moving windows to avoid noise from high-frequency variations in the parameter optimization that could induce convergence issues (Bacour et al., 2015). As far as test data from eddy-covariance measurements are concerned, high-frequency variations in fluxes also include variation in the boundary layer that are unrelated to the fluxes at the surface (Ibrom et al., 2006). Santaren, Peylin, Viovy, and Ciais (2007) estimated that for parameters related to photosynthesis and phenology, optimization based on half-hourly observations did not improve the results. For each site, the optimizations were conducted year by year to account for trait variability over time (Wu et al., 2013).

Following MacBean et al. (2015), each calibration (site-year) used 10 replicates representing different starting parameter sets, with values randomly picked within their allowed variation range (Supporting Information Appendix S1, Table S1.3). Only the best calibration out of these 10 replicates was retained for analyses. This procedure increases the chances of finding the global minimum of *J*, because Santaren et al. (2014) showed that the gradient-based algorithm was sensitive to initial conditions with a nonlinear and complex model, such as ORCHIDEE.

2.7 | Analyses

We retained only calibrations for which the optimized model reproduced GPP observations with high precision. The rationale for this was that optimized parameters from model runs that agreed poorly with GPP observations provided little or no useable information. The filtering was performed using a two-step procedure.

First, the criterion for "improved GPP simulation" was the relative site-year posterior Root Mean Square Error (RMSE) ($RMSE_{re}$) between observed and optimized GPP:

$$RMSE_{re} = \frac{RMSE}{\text{mean}\left(GPP_{obs}\right)} \tag{4}$$

Whenever the value of $RMSE_{re}$ was higher than the all-$RMSE_{re}$ median plus one interquartile range (IQR), the site-year was removed from the analysis. We also discarded sites with "inconsistent parameters values" [i.e., with too large differences between the 10 replicates at the same site, reflecting convergence issues (equifinality) of the algorithm].

Second, for sites with at least two $RMSE_{re}$ <10% among the 10 replicates, we estimated the coefficient of variation (CV) of parameters across the replicates. We retained only years for which the median CV was below the median of all CV plus one IQR of their distribution. This filtering provided optimized parameters from 371 site-years (of 516 considered initially) for 98 sites (of 116; Supporting Information Appendix S2) spanning seven PFTs located in boreal, temperate and tropical areas (Supporting Information Appendix S3, Table S3.4).

For each parameter, we calculated the uncertainty reduction (*UR*) as:

$$UR = 1 - \frac{\sigma_{post}}{\sigma_{prior}} \tag{5}$$

With σ_{post} and σ_{prior} being the *posterior* and *prior* parameter uncertainties (square root of the diagonal elements of *A* and *B*). We then separated in the analysis the well-constrained from the poorly constrained parameters. Well-constrained parameters are defined as those with: (a) *UR* higher than the median of *UR* distributions for all parameters; and (b) a low correlation of error with other parameters (from the *A* matrix; Equation 2). Note that a strong error correlation making two parameters poorly constrained individually is still an interesting result because it indicates a range of possible trade-offs between these two parameters.

The optimized parameter values were regressed against the local background bioclimatic variables (Table 2) for each site and against the soil relative water content (volume of water by volume of soil) simulated by ORCHIDEE. Bioclimatic variables were averaged over the whole year and over the length of the growing season (GSL). For temperate sites, the growing season was defined as the period with daily temperature >5°C and relative soil water content >0.2 (Violle et al., 2015). In some tropical regions, the growing season length is potentially limited by water availability (wet/dry seasons); we thus kept

TABLE 2 Description of bioclimatic variables calculated at each site and for each year

Variable	Description	Units
LAT	Latitude	Degrees north
MAT	Mean annual temperature	Degrees Celsius
TMAX	Mean temperature of the warmest month of the year	Degrees Celsius
TMIN	Mean temperature of the coldest month of the year	Degrees Celsius
TVAR	Temperature difference between *TMAX* and *TMIN*	Degrees Celsius
DTR	Yearly average of diurnal temperature range	Degrees Celsius
MAP	Mean annual precipitation	Millimetres per year
REH	Mean annual relative humidity	Percentage
SW	Mean annual downward shortwave radiation (visible and near-infrared)	Watts per square metre
PDRY	The driest quarter of the year is determined (to the nearest week), and the total precipitation over this period is calculated	Millimetres per year
RELP	*PDRY* divided by *MAP*	Fraction
SHUM	Yearly averaged soil humidity	Fraction
GSL	*MATgs*, *DTRgs*, *SWgs*, *MAPgs*, *REHgs* and *SHUMgs* are the same variables averaged during the growing season of the plant	–

the same definition as for temperate ecosystems. For boreal sites, we adapted the definition of the growing season such that weekly temperature must be >0°C.

Analyses were performed with the R v.3.2 software (R Core Team, 2016), and standardized major axis (SMA) analyses were performed with the "lmodel2" package (Legendre, 2014). Given that we sought to compare simulated correlations with common ecological properties observed at the global scale, we analysed different groups of PFTs: all PFTs together; deciduous versus evergreens; needleleaves versus broadleaves; and C_3 grasses (Supporting Information Appendix S1, Table S1.1). Regressions were performed both with and without a logarithmic transformation of the data.

3 | RESULTS AND COMPARISON TO EXISTING LITERATURE

3.1 | Optimization performances

A full description of the optimization performances and parameter uncertainty reduction can be found in the Supporting Information (Appendix S3).

In all cases, the optimized GPP time series agrees better with observations than the prior ones, with the RMSE being reduced by 76.6 ± 13.0% (Supporting Information Appendix S3, Table S3.4). The median posterior $RMSE_{re}$ is 0.19, and the IQR is 0.11. The median CV over all parameters is 0.24 (IQR = 0.13). After optimization, the parameter uncertainty (Equation 5) is reduced by 30% on average (Supporting Information Appendix S3, Table S3.5).

The posterior error correlation matrix *A* (Eq. 2) reveals a positive correlation between *Vcmax* and several other parameters, including (Figure 2): *Topt* (r = 0.57 ± 0.05); *gslope* (r = −0.37 ± 0.04); *Kroot* (r = 0.24 ± 0.07) and *Vj/Vc* (r = −0.31 ± 0.04). There also exists a negative correlation between *Kroot* and *gslope* (r = −0.38 ± 0.08), between *Kroot* and *Wlim* (r = −0.30 ± 0.09) and between *LAImax* and *Klai* (r = −0.37 ± 0.16) (Figure 2).

Joint analysis of information from the uncertainty reduction (Supporting Information Appendix S3) and the cross-parameter error correlation enables us to distinguish between: (a) well-constrained parameters (*Lage* and *SLA* for evergreens; *Lage* and *Csenes* for deciduous); (b) well-constrained parameters with a risk of equifinality (*gslope*, *Kroot*, *LAImax*, *Topt* and *Vcmax*); and (c) poorly constrained parameters (*Vj/Vc*, *Klai*, *Tauleaf* and *Wlim*; Table 1). In the following analyses, trait covariations have to be interpreted with respect to confidence intervals (posterior error) in parameter estimates.

3.2 | Covariation between parameters

We analysed cross-site correlations between optimized parameters in relationship to expected trait relationships. The covariation between all parameters is illustrated in the Supporting Information (Appendix S4, Figure S4.2). For more clarity and considering the large number of parameters, we describe here only the relationships involving four parameters related to phenology (*SLA*, *Lage*) and photosynthesis (*Vcmax*, *gslope*). All relationships are provided in the Supporting Information (Appendix S4, Table S4.6).

We observed a negative correlation between *SLA* and *Lage* for all PFTs (r = −0.63; Table 3) and for evergreens (r = −0.67) and broadleaves PFTs (r = −0.53), separately. The slope of the emerging relationship between *LMA* (1/*SLA*) and *Lage* (1.91; 1.63–2.24 95% confidence interval; $p < 0.05$) for all PFTs was close to the observed slope from field observations (1.71; 1.62–1.82; Wright et al., 2004). Results highlighted other covariations between *Lage* and *Vcmax* (r = −0.59 overall PFTs), *gslope* and *Lage* (r = −0.7 for broadleaves), *LAImax* and *SLA* (r = 0.6 for needleleaves), and *SLA* and *Vcmax* (r = −0.55 for evergreens). Here again, the slope between *Lage* and *Vcmax* emerging for broadleaves PFTs (−1.69) was close to observations (−1.13; Xu et al., 2017).

No relationships were reported between *gslope* and *Lage* or between *glsope* and *SLA*, but a trade-off between the stomatal conductance (*gs*) and *Lage* was observed experimentally (Poorter & Bongers, 2006; Reich, Walters, & Ellsworth, 1992), in addition to a positive correlation between *gs* and *SLA* (Poorter & Bongers, 2006). The optimizations showed opposite relationships between *gslope* and *SLA* depending on the PFT; a positive significant correlation was

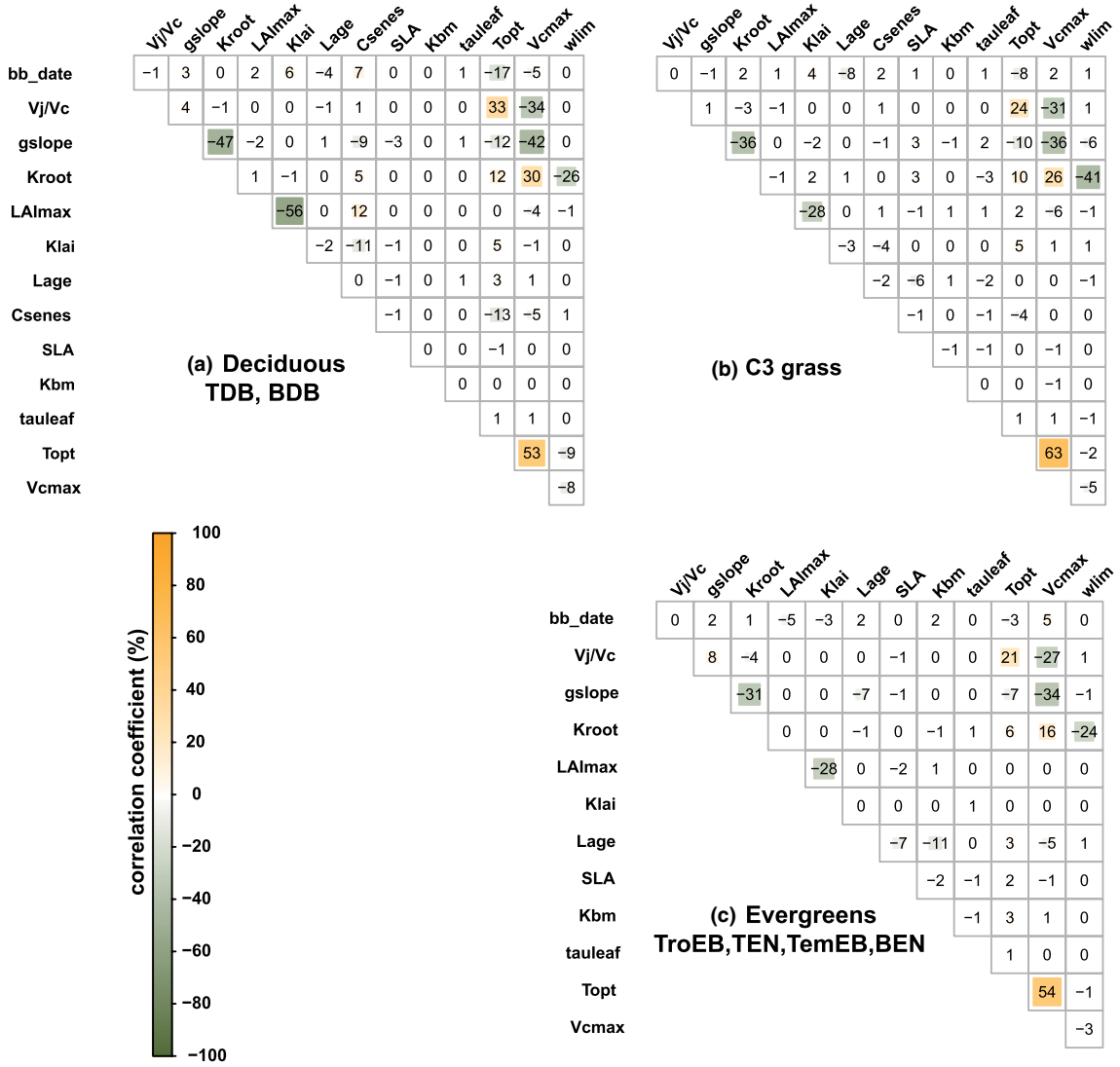

FIGURE 2 Error correlation between optimized parameters (derived from the *A* matrix) averaged over deciduous trees, evergreen trees and C_3 grass. The colour scale gives the error correlation coefficient. For greater clarity, the coefficient is indicated as a percentage in each matrix cell. A description of each parameter is listed in Table 1 [Colour figure can be viewed at wileyonlinelibrary.com]

obtained for deciduous PFTs and a negative significant correlation for evergreens and grasses (Table 3).

The positive relationship between *SLA* and *LAImax* emerging from optimized parameters for coniferous PFTs was consistent with the positive correlation between *LAI* and *SLA* reported by Pierce, Running, and Walker (1994) for coniferous forests. Finally, a negative correlation between *SLA* and *Vcmax* has been observed experimentally for two gymnosperm species (Niinemets, Lukjanova, Turnbull, & Sparrow, 2007), confirming the negative relationships found in our study for needleleaves. Despite the equifinality risk between *gslope* and the soil water stress, *Wlim*, in Figure 2, the positive correlation observed for broadleaves ($r = 0.7$) and evergreens ($r = 0.52$) was comparable to observations from independent data compiled by Lin et al. (2015).

Other significant correlations from the optimized parameters (Supporting Information Appendix S4, Table S4.6; Figure S4.2) could not be verified against observations because of the correlation of errors observed in Figure 2 or because of the scarcity of ecological data, preventing us from drawing a conclusion about the true nature of those correlations, such as between *gslope* and *Vcmax*.

3.3 | Variation of trait-related parameters with climate

We analysed correlations between parameters and climate variables (Table 4; Supporting Information Appendix S5, Figure S5.4). As for covariations between parameters, we described here only those involving *SLA*, *Lage*, *Vcmax* and *gslope*. All relationships are listed in the Supporting Information (Appendix S5, Table S5.7), and more detailed analyses are also available in the Supporting Information (Appendix S5).

We found a strong negative correlation between leaf lifespan (*Lage*) and temperatures (*MAT*, *TMIN*; $r = -0.78/-0.65$; Figure 3a) for evergreen PFTs. This correlation was reported independently at the global scale (van Ommen Kloeke et al., 2012; Wright et al., 2005)

TABLE 3 Relationships between trait-related parameters

Parameters		*r*	PFT	Log	SMA slope	Number of sites	References	Type
Lage	**SLA**	−0.67	ever	x	−1.39	49	Reich et al. (1999)	0
		−0.53	bro	x	−3.47	37		0
		−0.63	All	x	−1.92	98	Wright et al. (2004)	0
Lage	Vcmax	−0.90	Bro	x	−1.69	37	Xu et al. (2017)	0
		−0.65	Dec		−2.15	23		0
		−0.59	All	x	−3.13	98		0
gslope	**Lage**	−0.70	Bro	x	−0.74	37	Reich et al. (1992)	1
		−0.57	Grass		0.00	26	Poorter and Bongers (2006)	1
gslope	**SLA**	−0.62	Ever		−534.01	49	Poorter and Bongers (2006)	3
		0.52	Dec		418.99	23		1
		−0.51	Grass		−235.65	26		3
LAImax	**SLA**	0.60	Need		422.11	35	Pierce et al. (1994)	1
SLA	Vcmax	−0.55	Ever	x	−1.28	49	Niinemets et al. (2007)	1
		−0.53	Need	x	−0.75	35		1
gslope	*Wlim*	0.70	Bro	x	1.61	37	Lin et al. (2015)	3
		0.52	Ever	x	1.47	49		3

Note: For some relationships, values are $\log_{10}$-transformed (x). For each relationship is shown the number of sites and the correlation coefficient (*r*; blue when negative; red when positive). Only relationships with an absolute and significant ($p < 0.05$) correlation coefficient >0.5 are listed for the different groups of plant functional type (PFT): all, broadleaves (bro; TroEB, TemEB, TDB and BDB), needleleaves (need; TEN and BEN), evergreens (ever; TroEB, TemEB, TEN and BEN), deciduous (dec; TDB and BDB) and C_3 grasses (gra). Note that evergreens include needleleaves and that broadleaves include deciduous. The type of relationship is given for each trait: 0 = verified with ecological observations; 1 = partly verified on similar data; or 3 = different from observations. When available, the reference for verification is given. Well-constrained parameters are in bold, parameters with a risk of equifinality are in plain text, and poorly constrained parameters are in italic. Refer to Table 1 for the description of each parameter.

and confirmed by Reich, Rich, Lu, Wang, and Oleksyn (2014), who showed higher needle longevity with cold temperatures for boreal species. However, the observed positive correlation between *Lage* and *MAT* at the global scale for deciduous PFTs (van Ommen Kloeke et al., 2012; Wright et al., 2005) was not found specifically for deciduous systems in our study. Nevertheless, a positive correlation was observed for C_3 grasses and broadleaves (including deciduous). We also found a strong negative correlation between *Lage* and the mean annual precipitations (*MAP*) for evergreen PFTs ($r = -0.65$), consistent with field data (van Ommen Kloeke et al., 2012). In addition, a negative correlation between *Lage* and incident shortwave radiation (*SW*) for evergreens was obtained, consistent with field observations (Poorter & Bongers, 2006).

Regarding *SLA*, we found opposite sensitivities to *MAT* for evergreen ($r = 0.65$) and deciduous forests ($r = -0.55$). This result is consistent with independent leaf-scale data showing a positive correlation between *SLA* and *MAT* for evergreen species (Figure 3b) and a negative correlation for deciduous species (Wright et al., 2005). The model calibration also resulted in a positive correlation between the relative precipitation (*RELP*; Table 2) and *SLA* for deciduous trees ($r = 0.60$; Figure 3c). Regarding the positive correlations obtained between *SLA* with *Kroot* or *gslope* (Table 3), it suggests that *SLA* is highly sensitive to water stress for deciduous trees. For evergreens, a positive correlation between *SLA* and precipitation also emerges when considering the length of the growing season (*MAPgs*, $r = 0.57$; Table 4), which is consistent with trait data (Wright et al., 2005). For evergreens, *SLA* was positively correlated with *SW* ($r = 0.53$), a relationship observed by Givnish, Montgomery, and Goldstein (2004) and Poorter and Bongers (2006).

In their meta-analysis of stomatal conductance parameters from observations of several PFTs, Lin et al. (2015) showed that the slope of the stomatal conductance is positively correlated with the mean air temperature over the growing period and with soil moisture stress. Here, our results show the same correlation between *gslope* and soil moisture during the growing season ($r = 0.71$; Figure 3d) and relative precipitation ($r = 0.66$) for deciduous or broadleaved PFTs. On the contrary, we find that *gslope* is negatively correlated with mean annual precipitation for C_3 grasses ($r = -0.59$) and with shortwave radiation for broadleaved PFTs ($r = -0.63$). Medlyn et al. (2011) suggested that *gslope* is proportional to the photosynthesis compensation point for CO_2 and, consequently, to growth temperatures of the plant (Bernacchi, Singsaas, Pimentel, Portis, & Long, 2001). This assumption is supported by the data from Lin et al. (2015). In our study, the relationship between *gslope* and temperature was not supported.

Finally, *Vcmax* is mostly sensitive to temperature and light for broadleaved PFTs, with a negative correlation observed with *MAT* ($r = -0.52$) and *SW* ($r = -0.54$). This result contradicts previous observations by Ali et al. (2015), who suggested a positive correlation between *Vcmax* and seasonal temperature and light variations.

TABLE 4 Relationships between trait-related parameters and climate variables

Trait	Climate	*r*	PFT	Log	SMA slope	References	Type
Lage	*LAT*	0.59	ever		24.90	Reich et al. (2014)	0
		−0.56	bro		−13.44		2
	MAP	0.66	grass		1.14		2
		−0.65	need	x	−0.66	van Ommen Kloeke et al. (2012)	0
	MAT	−0.78	ever	x	−16.95	Reich et al. (2014); van Ommen Kloeke et al. (2012); Wright et al. (2005)	0
		−0.62	need	x	−17.93		0
		0.54	grass	x	107.81		2
		0.53	bro	x	30.14		2
	SW	−0.53	ever	x	−1.84	Poorter and Bongers (2006)	1
		0.52	bro	x	3.85		2
	TMIN	−0.65	ever	x	−30.99	Reich et al. (2014); van Ommen Kloeke et al. (2012); Wright et al. (2005)	1
SLA	*MAP*	0.54	need	x	0.37	Wright et al. (2005)	0
	MAPgs	0.57	ever	x	0.47		0
	MAT	0.65	ever	x	12.16	Wright et al. (2005)	0
	MATgs	−0.63	bro	x	−0.86		0
		−0.55	dec	x	−0.96		0
	RELP	0.60	dec	x	0.25		2
		0.59	bro		0.08		2
	SW	0.53	ever		0.00	Givnish et al. (2004); Poorter and Bongers (2006); Reich et al. (2014)	1
gslope	*MAP*	−0.59	grass	x	−1.12		2
	PDRY	0.58	dec		0.02	Lin et al. (2015)	1
	REH	0.64	dec		19.24		1
	RELP	0.66	bro		42.67		1
		0.58	dec		29.05		1
	SHUMgs	0.71	dec		20.53		1
	SW	−0.63	bro		−0.10		2
	SWgs	−0.55	dec		−0.08		2
Vcmax	*MAT*	−0.52	bro		−4.77	Ali et al. (2015)	3
	RELP	0.60	bro		511.72		2
	SW	−0.54	bro		−1.15	Ali et al. (2015)	3

Note: For some relationships, traits values are $\log_{10}$-transformed (x). For each relationship, the correlation coefficient (*r*) is given. Only relationships with an absolute (and significant *p*-value < 0.05) correlation coefficient >0.5 are listed for the different groups of plant functional type (PFT): all, broadleaves (bro; TroEB, TemEB, TDB and BDB), needleleaves (need; TEN and BEN), evergreens (ever; TroEB, TemEB, TEN and BEN), deciduous (dec; TDB and BDB) and C_3 grasses (gra). The type of relationship is given for each trait: 0 = verified with ecological observations; 1 = partly verified on similar data; 2 = not verified; or 3 = different from observations. When available, the reference for verification is given. Well-constrained parameters are in bold, and parameters with a risk of equifinality are in plain text. See Table 1 and 2 for the description of each parameter and climate variables, respectively.

4 | DISCUSSION

4.1 | Uncertainties and shortcomings of the approach

This section provides an overview of possible shortcomings of our approach that might explain some residual mismatch between the model and observations. Several factors can impact the optimized value of the parameters, potentially aliasing the observed relationships: (a) flux measurement errors and errors in ecosystem respiration estimates used to derive gap-filled GPP; (b) optimization protocol/set-up errors; and (c) model systematic errors deriving from absent or poorly represented processes in the model.

First, we restricted our analysis to GPP. This flux is not measured directly but estimated from NEE measured using the eddy-covariance method, with an estimate of ecosystem respiration determined using empirical models (Reichstein et al., 2005), and thus can be

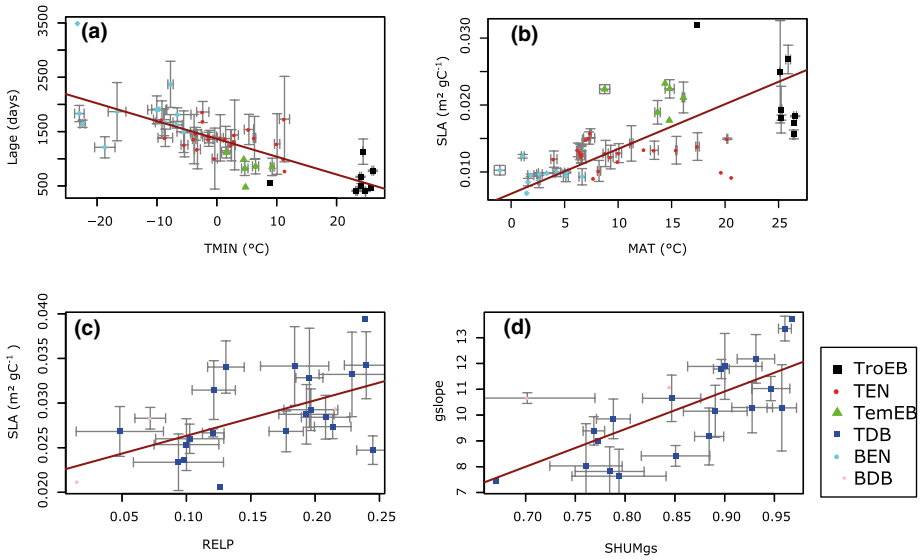

FIGURE 3 Four examples of covariations obtained between optimized parameters (Table 1) and environmental conditions (Table 2) of the sites for plant functional types (PFTs) TroEB (black square), TEN (red square), TemEB (green triangle), TDB (blue square), BEN (cyan dots) and BDB (pink dots). Each point represents the mean optimized parameter (environmental variable) value for one site, and the error bars represent the inter-annual variability (no bars means only 1 year of measurement). The red line represents the slope of the standardized major axis regression. PFT description can be found in Table S1.1 (Appendix S1) [Colour figure can be viewed at wileyonlinelibrary.com]

biased by several factors (for a list of these factors, see Supporting Information Appendix S3). We chose GPP over a combination of NEE and latent heat or evapotranspiration fluxes, which has often been used to optimize ORCHIDEE (Bacour et al., 2015; Kuppel et al., 2012; Peylin et al., 2016), because it implies the optimization of more parameters related to soil, respiration and energy budget, and therefore increases the risk of equifinality. To reduce the uncertainties, it is necessary to lower the correlation of errors between parameters by assimilating complementary biophysical variables. For example, assimilating both GPP and LAI estimates at the site level could improve the evaluation of parameters such as *SLA* or *Lage* and, consequently, improve the estimation of photosynthesis parameters.

Second, the Bayesian framework is based on the assumption that the model/observation errors are random and that the model structure is "true". Any bias of model structure is expected to be aliased onto the estimated parameters (MacBean, Peylin, Chevallier, Scholze, & Schürmann, 2016) and might therefore impact the retrieved correlations. For instance, missing processes would be compensated during the optimization by adjusting parameters (e.g., light attenuation, vertical distribution of leaf area index, diffuse light, horizontal light distribution in the stand) to non-optimal values. Also, although traits are usually measured at the leaf level, our approach rather focuses on traits at the canopy level [given the structure of ORCHIDEE and the assumed exponential attenuation of light and leaf area index from top to bottom of canopy (Krinner et al., 2005; Supporting Information Appendix S1, Table S1.2) and the assimilation of GPP data]. As an additional test, we conducted the above analyses using multi-year instead of single-year observations in order to add more constraints on parameters (see Supporting Information Appendix S4, Figures S4.3 and S5.5). The same relationships were found as with single-year observations, thus strengthening our conclusions, showing that spatial correlations are observed even when taking into account a possible temporal variability of traits.

Finally, an incorrect representation of species and the lack of representation of variability of traits within a community in ORCHIDEE can affect simulated processes, which will ultimately impact the estimated parameter values (for a discussion on initial site conditions, see Supporting Information Appendix S3). Especially, the C_3 grass PFT represents diverse grasslands, with different species, ecophysiology (Adams, Turnbull, Sprent, & Buchmann, 2016) and management practices (Merbold et al., 2014). This results in an increased variability and a high range of estimated plant functional traits (Supporting Information Appendix S3, Figure S3.1). A refinement of the PFT definition might improve the robustness of optimizations (for instance, by separating natural or semi-managed biomes or by distinguishing genera or major species; Peaucelle et al., 2017).

In order to decrease the impact of uncertainty in PFT composition and reduce the correlation errors between parameters, the use of concomitant observations of traits and carbon fluxes at the FLUXNET sites would enable: (a) the constraint of known parameters; and (b) the validation of optimized traits. However, functional trait observations at FLUXNET sites and a precise description of species composition are not yet systematic (Musavi et al., 2015, 2016).

4.2 | Ecological consistency of trait relationships

The optimization of model parameters managed to reproduce many known ecological properties. The optimized parameters consistently matched the well-known relationships resulting from the leaf economic spectrum (LES) theory (Reich et al., 1999; Wright et al., 2004).

In particular, our results align with the trait theory that long-lived canopies are metabolically less active and are consistent with the LES empirical evidence that plants invest either in structure or in photosynthesis (Liu et al., 2010; Reich, 2014).

Our results also reproduced several observed trait–climate relationships at the PFT level. Globally, evergreen PFT parameters showed a strong dependence on mean annual temperature and radiation, whereas parameters for deciduous PFTs exhibited a strong sensitivity to precipitation and soil moisture over the growing season (Supporting Information Appendix S5, Figure S5.4). As postulated by Reich (2014), climate exerts a control on the average leaf characteristics at the community level. The observed relationships obtained at the PFT level might reflect not only differences in plant response to climate, but also differences in plant community composition (Shi et al., 2015). These results suggest that both the development of acclimation processes and trait-based approaches are needed in TBMs if we seek to capture the effect of biogeography on ecosystem characteristics (Fisher et al., 2018; Lu et al., 2017).

Finally, although the results clearly highlight that photosynthesis and phenological mechanisms implemented in ORCHIDEE are robust enough to reproduce known behaviours of several vegetation species, below-ground processes still appear poorly represented, which resulted in weakly constrained parameters and trait covariations inconsistent with the literature. These discrepancies are primarily attributable to a lack of ecophysiological knowledge that reflects the difficulty of studying below-ground ecological processes. The rooting system uses model-specific parameters (*Kroot*) that are hardly comparable to measured functional traits.

5 | CONCLUDING REMARKS AND RECOMMENDATIONS

The approach presented in this study is a new and effective way to validate the processes implemented in TBMs, to provide a better definition of vegetation response to climate (Liang et al., 2018), and could help to improve existing data assimilation frameworks (Arsenault et al., 2018; Kaminski et al., 2013; LeBauer, Wang, Richter, Davidson, & Dietze, 2013) by providing ecological constraints. The availability of continuous observations from eddy-covariance flux measurements gives a unique opportunity to resolve the different components of the short- and long-term variability of traits through this approach.

Our results show that optimized leaf-related parameters align with plant trait theory and highlight the need to implement acclimation processes and trait-based approaches in models instead of using constant parameters to reduce uncertainties in spatio-temporal patterns of the modelled carbon fluxes. A first step would be to assess the behaviour of the model at the global scale when trait–climate relationships characterized in this study are implemented explicitly. In parallel, the relationships highlighted in the present study might help in development or validation of new methods to simulate plant acclimation. Used in a prognostic way, this approach could enable the study of correlations at the canopy scale and assessment of the behaviour of trait-related parameters that are difficult to observe experimentally.

Several known ecological properties, observed at the site/leaf scale, emerged from model–data assimilation. However, quantitative comparisons with observations were possible only for two of them, *SLA* and *Lage*, which are also the two most studied traits. This is mainly because TBMs use model-specific parameters that cannot be compared directly with standard trait observations, but also because concomitant observations of functional traits, both in space and in time, are scarce in the literature. A recommendation to the TBM community would be to make use of parameters (and processes) that can be related directly to observations in order to unite vegetation model and functional traits (for instance, the use of the specific root length for below-ground processes).

We argue that co-located systematic and standardized trait observations [starting with key traits related to phenology (*SLA* and *LAI*), photosynthesis (*Vcmax*, *Jmax* and *Topt*), water transport (*gs*) and allocation (*carbon:nitrogen ratio* and *shoot/root*); Law et al., 2008] along with biometric data are needed at the FLUXNET sites or within other environmental observation networks, such as Integrated Carbon Observation System (ICOS) or National Ecological Observatory Network (NEON), if we seek to distinguish temporal and spatial components of trait variability across biomes and climates. The creation of a FLUXNET trait database could improve our comprehension of trait acclimation and help us to disentangle the differences observed at regional and local scales, to improve the scaling up of processes from the leaf to the canopy/ecosystem level and to calibrate/validate ecosystem models properly.

ACKNOWLEDGMENTS

This work was performed using HPC resources from GENCI-TGCC (grant 2017-A0030106328). The authors would like to acknowledge the financial support from the European Research Council Synergy grant ERC-SyG-2013-610028 IMBALANCE-P. The study was supported by the National Centre of Excellence (272041), ICOS-Finland (281255) and Academy professor project (284701) funded by the Academy of Finland. N.B. acknowledges various funding sources for the Swiss FluxNet, particularly from the Swiss National Science Fundation (SNF) (grants: 20FI21_148992, 20FI20_173691). L.M. was supported by the Swiss National Science Foundation under the 40FA40_154245/1 grant agreement. This work used eddy-covariance data acquired and shared by the FLUXNET community, including these networks: AmeriFlux, AfriFlux, AsiaFlux, CarboAfrica, CarboEuropeIP, CarboItaly, CarboMont, ChinaFlux, Fluxnet-Canada, GreenGrass, Integrated Carbon Observation System (ICOS), KoFlux, LBA, NECC, OzFlux-TERN, TCOS-Siberia and USCCC. The ERA-Interim reanalysis data are provided by European Centre for Medium-Range Weather Forecasts (ECMWF) and processed by Laboratoire des Sciences du Climat et de l'Environnement (LSCE). The FLUXNET eddy-covariance data processing and harmonization were carried out by the European Fluxes Database Cluster, AmeriFlux Management Project and Fluxdata project of FLUXNET, with the support of Carbon Dioxide Information Analysis Center (CDIAC) and ICOS Ecosystem Thematic Center, and the OzFlux, ChinaFlux and AsiaFlux offices. L.B.M. acknowledges the support of the RUDN University program 5-100. L.Š. was supported by

the Ministry of Education, Youth and Sports of CR within the National Sustainability Program I (NPU I), grant number LO1415.

DATA ACCESSIBILITY

All FluxNet data can be downloaded at: https://fluxnet.fluxdata.org. Information about the ORCHIDEE model, source code and contact: http://orchidee.ipsl.fr/. Information about the data assimilation system ORCHIDAS: https://orchidas.lsce.ipsl.fr/. Information about the HWSD v1.2: http://webarchive.iiasa.ac.at/Research/LUC/External-World-soil-database/HTML/

ORCID

Marc Peaucelle https://orcid.org/0000-0003-0324-4628
Philippe Ciais https://orcid.org/0000-0001-8560-4943
Sylvain Kuppel https://orcid.org/0000-0003-3632-2100
Josep Peñuelas https://orcid.org/0000-0002-7215-0150
Luca Belelli Marchesini https://orcid.org/0000-0001-8408-4675
Peter D. Blanken https://orcid.org/0000-0002-7405-2220
Nina Buchmann https://orcid.org/0000-0003-0826-2980
Jiquan Chen https://orcid.org/0000-0003-0761-9458
Nicolas Delpierre https://orcid.org/0000-0003-0906-9402
Ankur R. Desai https://orcid.org/0000-0002-5226-6041
Damiano Gianelle https://orcid.org/0000-0001-7697-5793
Cristina Gimeno-Colera https://orcid.org/0000-0001-9532-5577
Carsten Gruening https://orcid.org/0000-0002-6169-2827
Carole Helfter https://orcid.org/0000-0001-5773-4652
Lukas Hörtnagl https://orcid.org/0000-0002-5569-0761
Andreas Ibrom https://orcid.org/0000-0002-1341-921X
Richard Joffre https://orcid.org/0000-0001-8205-7710
Tomomichi Kato https://orcid.org/0000-0003-3757-3243
Beverly Law https://orcid.org/0000-0002-1605-1203
Anders Lindroth https://orcid.org/0000-0002-7669-784X
Ivan Mammarella https://orcid.org/0000-0002-8516-3356
Lutz Merbold https://orcid.org/0000-0003-4974-170X
Stefano Minerbi https://orcid.org/0000-0002-6620-2735
Leonardo Montagnani https://orcid.org/0000-0003-2957-9071
Ladislav Šigut https://orcid.org/0000-0003-1951-4100
Andrej Varlagin https://orcid.org/0000-0002-2549-5236
Timo Vesala https://orcid.org/0000-0002-4852-7464
Georg Wohlfahrt https://orcid.org/0000-0003-3080-6702
Sebastian Wolf https://orcid.org/0000-0001-7717-6993
Dan Yakir https://orcid.org/0000-0003-3381-1398
Nicolas Viovy https://orcid.org/0000-0002-9197-6417

REFERENCES

Adams, M. A., Turnbull, T. L., Sprent, J. I., & Buchmann, N. (2016). Legumes are different: Leaf nitrogen, photosynthesis, and water use efficiency. *Proceedings of the National Academy of Sciences USA*, *113*, 4098–4103.

Ali, A. A., Xu, C., Rogers, A., McDowell, N. G., Medlyn, B. E., Fisher, R. A., … Santiago, L. S. (2015). Global-scale environmental control of plant photosynthetic capacity. *Ecological Applications*, *25*, 2349–2365.

Arsenault, K. R., Kumar, S. V., Geiger, J. V., Wang, S., Kemp, E., Mocko, D. M., … Jacob, J. (2018). The Land surface Data Toolkit (LDT v7. 2) – A data fusion environment for land data assimilation systems. *Geoscientific Model Development*, *11*, 3605–3621.

Atkin, O. K., Bloomfield, K. J., Reich, P. B., Tjoelker, M. G., Asner, G. P., Bonal, D., … Zaragoza-Castells, J. (2015). Global variability in leaf respiration in relation to climate, plant functional types and leaf traits. *New Phytologist*, *206*, 614–636.

Azevedo, G., & Marenco, R. (2012). Growth and physiological changes in saplings of *Minquartia guianensis* and *Swietenia macrophylla* during acclimation to full sunlight. *Photosynthetica*, *50*, 86–94.

Bacour, C., Peylin, P., MacBean, N., Rayner, P., Delage, F., Chevallier, F., … Berveiller, F. (2015). Joint assimilation of eddy covariance flux measurements and FAPAR products over temperate forests within a process-oriented biosphere model. *Journal of Geophysical Research: Biogeosciences*, *120*, 1839–1857.

Bernacchi, C. J., Singsaas, E. L., Pimentel, C., Portis, A. R., Jr., & Long, S. P. (2001). Improved temperature response functions for models of Rubisco-limited photosynthesis. *Plant, Cell & Environment*, *24*, 253–259.

Bjorkman, A. D., Myers-Smith, I. H., Elmendorf, S. C., Normand, S., Thomas, H. J., Alatalo, J. M., … Baruah, G. (2018). Tundra Trait Team: A database of plant traits spanning the tundra biome. *Global Ecology and Biogeography*, *27*, 1402–1411.

Botta, A., Viovy, N., Ciais, P., Friedlingstein, P., & Monfray, P. (2000). A global prognostic scheme of leaf onset using satellite data. *Global Change Biology*, *6*, 709–725.

Byrd, R. H., Lu, P., Nocedal, J., & Zhu, C. (1995). A limited memory algorithm for bound constrained optimization. *SIAM Journal on Scientific Computing*, *16*, 1190–1208.

Carvalhais, N., Reichstein, M., Ciais, P., Collatz, G. J., Mahecha, M. D., Montagnani, L., … Seixas, J. (2010). Identification of vegetation and soil carbon pools out of equilibrium in a process model via eddy covariance and biometric constraints. *Global Change Biology*, *16*, 2813–2829.

Cernusak, L. A., Hutley, L. B., Beringer, J., Holtum, J. A., & Turner, B. L. (2011). Photosynthetic physiology of eucalypts along a sub-continental rainfall gradient in northern Australia. *Agricultural and Forest Meteorology*, *151*, 1462–1470.

Dee, D., Uppala, S., Simmons, A., Berrisford, P., Poli, P., Kobayashi, S., … Bechtold, P. (2011). The ERA-Interim reanalysis: Configuration and performance of the data assimilation system. *Quarterly Journal of the Royal Meteorological Society*, *137*, 553–597.

Deng, X., Ye, W.-H., Feng, H.-L., Yang, Q.-H., Cao, H.-L., Xu, K.-Y., & Zhang, Y. (2004). Gas exchange characteristics of the invasive species *Mikania micrantha* and its indigenous congener *M. cordata* (Asteraceae) in South China. *Botanical Bulletin of Academia Sinica*, *45*, 213–220.

Domingues, T. F., Meir, P., Feldpausch, T. R., Saiz, G., Veenendaal, E. M., Schrodt, F., … Lloyd, J. (2010). Co-limitation of photosynthetic capacity by nitrogen and phosphorus in West Africa woodlands. *Plant, Cell & Environment*, *33*, 959–980.

Ducoudré, N. I., Laval, K., & Perrier, A. (1993). SECHIBA, a new set of parameterizations of the hydrologic exchanges at the land-atmosphere interface within the LMD atmospheric general circulation model. *Journal of Climate*, *6*, 248–273.

Fisher, J. B., Badgley, G., & Blyth, E. (2012). Global nutrient limitation in terrestrial vegetation. *Global Biogeochemical Cycles*, *26*, GB3007.

Fisher, R. A., Koven, C. D., Anderegg, W. R., Christoffersen, B. O., Dietze, M. C., Farrior, C. E., … Lichstein, J. W. (2018). Vegetation demographics in Earth System Models: A review of progress and priorities. *Global Change Biology*, *24*, 35–54.

Givnish, T. J., Montgomery, R. A., & Goldstein, G. (2004). Adaptive radiation of photosynthetic physiology in the Hawaiian lobeliads: Light regimes, static light responses, and whole-plant compensation points. *American Journal of Botany*, *91*, 228–246.

Hartig, F., Dyke, J., Hickler, T., Higgins, S. I., O'Hara, R. B., Scheiter, S., & Huth, A. (2012). Connecting dynamic vegetation models to data–an inverse perspective. *Journal of Biogeography*, *39*(12), 2240–2252.

Ibrom, A., Jarvis, P. G., Clement, R., Morgenstern, K., Oltchev, A., Medlyn, B. E., … Gravenhorst, G. (2006). A Comparative analysis of simulated and observed photosynthetic CO_2 uptake in two coniferous forest canopies. *Tree Physiology*, *26*, 845–864.

Kaminski, T., Knorr, W., Schürmann, G., Scholze, M., Rayner, P., Zaehle, S., … Gobron, N. (2013). The BETHY/JSBACH carbon cycle data assimilation system: Experiences and challenges. *Journal of Geophysical Research: Biogeosciences*, *118*, 1414–1426.

Kattge, J., Díaz, S., Lavorel, S., Prentice, I. C., Leadley, P., Bönisch, G., … Wirth, C. (2011). TRY – a global database of plant traits. *Global Change Biology*, *17*, 2905–2935.

Kattge, J., Knorr, W., Raddatz, T., & Wirth, C. (2009). Quantifying photosynthetic capacity and its relationship to leaf nitrogen content for global-scale terrestrial biosphere models. *Global Change Biology*, *15*, 976–991.

Krinner, G., Viovy, N., de Noblet-Ducoudré, N., Ogée, J., Polcher, J., Friedlingstein, P., … Prentice, I. C. (2005). A dynamic global vegetation model for studies of the coupled atmosphere-biosphere system. *Global Biogeochemical Cycles*, *19*, 33 p.

Kroner, Y., & Way, D. A. (2016). Carbon fluxes acclimate more strongly to elevated growth temperatures than to elevated CO_2 concentrations in a northern conifer. *Global Change Biology*, *22*, 2913–2928.

Kuppel, S. (2012). *Assimilation de mesures de flux turbulents d'eau et de carbone dans un modèle de la biosphère continentale*. Versailles: St Quentin en Yvelines.

Kuppel, S., Peylin, P., Chevallier, F., Bacour, C., Maignan, F., & Richardson, A. (2012). Constraining a global ecosystem model with multi-site eddy-covariance data. *Biogeosciences*, *9*, 3757–3776.

Kuppel, S., Peylin, P., Maignan, F., Chevallier, F., Kiely, G., Montagnani, L., & Cescatti, A. (2014). Model–data fusion across ecosystems: From multisite optimizations to global simulations. *Geoscientific Model Development*, *7*, 2581–2597.

Lardy, R., Bellocchi, G., & Soussana, J.-F. (2011). A new method to determine soil organic carbon equilibrium. *Environmental Modelling & Software*, *26*, 1759–1763.

Law, B. E., Arkebauer, T., Campbell, J. L., Chen, J., Sun, O., Schwartz, M., … Verma, S. (2008). *Terrestrial carbon observations: Protocols for vegetation sampling and data submission*. Rome: FAO.

LeBauer, D. S., Wang, D., Richter, K. T., Davidson, C. C., & Dietze, M. C. (2013). Facilitating feedbacks between field measurements and ecosystem models. *Ecological Monographs*, *83*, 133–154.

Legendre, P. (2014) *lmodel2: Model II Regression. R package version 1.7-2*. Retrieved from http://CRAN.R-project.org/package=lmodel2

Liang, J., Xia, J., Shi, Z., Jiang, L., Ma, S., Lu, X., … Penton, C. R. (2018). Biotic responses buffer warming-induced soil organic carbon loss in Arctic tundra. *Global Change Biology*, *24*, 4946–4959.

Lin, Y.-S., Medlyn, B. E., Duursma, R. A., Prentice, I. C., Wang, H., Baig, S., … De Beeck, M. O. (2015). Optimal stomatal behaviour around the world. *Nature Climate Change*, *5*, 459–464.

Liu, G., Freschet, G. T., Pan, X., Cornelissen, J. H. C., Li, Y., & Dong, M. (2010). Coordinated variation in leaf and root traits across multiple spatial scales in Chinese semi-arid and arid ecosystems. *New Phytologist*, *188*, 543–553.

Luo, Y., Jiang, L., Niu, S., & Zhou, X. (2017). Nonlinear responses of land ecosystems to variation in precipitation. *New Phytologist*, *214*, 5–7.

Lu, X., Wang, Y.-P., Wright, I. J., Reich, P. B., Shi, Z., & Dai, Y. (2017). Incorporation of plant traits in a land surface model helps explain the global biogeographical distribution of major forest functional types. *Global Ecology and Biogeography*, *26*, 304–317.

MacBean, N., Maignan, F., Peylin, P., Bacour, C., Bréon, F.-M., & Ciais, P. (2015). Using satellite data to improve the leaf phenology of a global terrestrial biosphere model. *Biogeosciences*, *12*, 7185–7208.

MacBean, N., Peylin, P., Chevallier, F., Scholze, M., & Schürmann, G. (2016). Consistent assimilation of multiple data streams in a carbon cycle data assimilation system. *Geoscientific Model Development*, *9*, 3569–3588.

Maire, V., Wright, I. J., Prentice, I. C., Batjes, N. H., Bhaskar, R., Bodegom, P. M., … Reich, P. B. (2015). Global effects of soil and climate on leaf photosynthetic traits and rates. *Global Ecology and Biogeography*, *24*, 706–717.

Medlyn, B. E., Duursma, R. A., Eamus, D., Ellsworth, D. S., Prentice, I. C., Barton, C. V. M., … Wingate, L. (2011). Reconciling the optimal and empirical approaches to modelling stomatal conductance. *Global Change Biology*, *17*, 2134–2144.

Meir, P., Levy, P. E., Grace, J., & Jarvis, P. G. (2007). Photosynthetic parameters from two contrasting woody vegetation types in West Africa. *Plant Ecology*, *192*, 277–287.

Merbold, L., Eugster, W., Stieger, J., Zahniser, M., Nelson, D., & Buchmann, N. (2014). Greenhouse gas budget (CO_2, CH_4 and N_2O) of intensively managed grassland following restoration. *Global Change Biology*, *20*, 1913–1928.

Musavi, T., Mahecha, M. D., Migliavacca, M., Reichstein, M., van de Weg, M. J., van Bodegom, P. M., … Schrodt, F. (2015). The imprint of plants on ecosystem functioning: A data-driven approach. *International Journal of Applied Earth Observation and Geoinformation*, *43*, 119–131.

Musavi, T., Migliavacca, M., van de Weg, M. J., Kattge, J., Wohlfahrt, G., van Bodegom, P. M., … Mahecha, M. D. (2016). Potential and limitations of inferring ecosystem photosynthetic capacity from leaf functional traits. *Ecology and Evolution*, *6*, 7352–7366.

Nachtergaele, F. O., van Velthuizen, H., Verelst, L., Wiberg, D., Batjes, N. H., Dijkshoorn, J. A., … Shi, X. (2012). *Harmonized World Soil Database* (version 1.2), 42.

Nascimento, H. C., & Marenco, R. A. (2013). Mesophyll conductance variations in response to diurnal environmental factors in *Myrcia paivae* and *Minquartia guianensis* in Central Amazonia. *Photosynthetica*, *51*, 457–464.

Niinemets, Ü., Lukjanova, A., Turnbull, M. H., & Sparrow, A. D. (2007). Plasticity in mesophyll volume fraction modulates light-acclimation in needle photosynthesis in two pines. *Tree Physiology*, *27*, 1137–1151.

Niinemets, Ü., Oja, V., & Kull, O. (1999). Shape of leaf photosynthetic electron transport versus temperature response curve is not constant along canopy light gradients in temperate deciduous trees. *Plant, Cell & Environment*, *22*, 1497–1513.

Ordoñez, J. C., Van Bodegom, P. M., Witte, J.-P. M., Wright, I. J., Reich, P. B., & Aerts, R. (2009). A global study of relationships between leaf traits, climate and soil measures of nutrient fertility. *Global Ecology and Biogeography*, *18*, 137–149.

Pavlick, R., Drewry, D. T., Bohn, K., Reu, B., & Kleidon, A. (2013). The Jena Diversity-Dynamic Global Vegetation Model (JeDi-DGVM): A diverse approach to representing terrestrial biogeography and biogeochemistry based on plant functional trade-offs. *Biogeosciences*, *10*, 4137–4177.

Peaucelle, M., Bellassen, V., Ciais, P., Peñuelas, J., & Viovy, N. (2017). A new approach to optimal discretization of plant functional types in a process-based ecosystem model with forest management: a case study for temperate conifers. *Global Ecology and Biogeography*, *26*, 486–499.

Peylin, P., Bacour, C., MacBean, N., Leonard, S., Rayner, P. J., Kuppel, S., … Prunet, P. (2016). A new step-wise Carbon Cycle Data Assimilation System

using multiple data streams to constrain the simulated land surface carbon cycle. *Geoscientific Model Development Discussions*, *9*, 3321–3356.

Pierce, L. L., Running, S. W., & Walker, J. (1994). Regional-scale relationships of leaf area index to specific leaf area and leaf nitrogen content. *Ecological Applications*, *4*, 313–321.

Poorter, L., & Bongers, F. (2006). Leaf traits are good predictors of plant performance across 53 rain forest species. *Ecology*, *87*, 1733–1743.

Prentice, I. C., Dong, N., Gleason, S. M., Maire, V., & Wright, I. J. (2014). Balancing the costs of carbon gain and water transport: Testing a new theoretical framework for plant functional ecology. *Ecology Letters*, *17*, 82–91.

R Core Team, D. (2016). *R: A language and environment for statistical computing*. Vienna, Austria: R Foundation for Statistical Computing.

Reich, P. B. (2014). The world-wide 'fast–slow' plant economics spectrum: A traits manifesto. *Journal of Ecology*, *102*, 275–301.

Reich, P. B., Ellsworth, D. S., Walters, M. B., Vose, J. M., Gresham, C., Volin, J. C., & Bowman, W. D. (1999). Generality of leaf trait relationships: A test across six biomes. *Ecology*, *80*, 1955–1969.

Reich, P. B., Rich, R. L., Lu, X., Wang, Y.-P., & Oleksyn, J. (2014). Biogeographic variation in evergreen conifer needle longevity and impacts on boreal forest carbon cycle projections. *Proceedings of the National Academy of Sciences USA*, *111*, 13703–13708.

Reich, P. B., Sendall, K. M., Stefanski, A., Wei, X., Rich, R. L., & Montgomery, R. A. (2016). Boreal and temperate trees show strong acclimation of respiration to warming. *Nature*, *531*, 633–636.

Reich, P. B., Walters, M. B., & Ellsworth, D. S. (1992). Leaf life-span in relation to leaf, plant, and stand characteristics among diverse ecosystems. *Ecological Monographs*, *62*, 365–392.

Reich, P. B., Wright, I. J., & Lusk, C. H. (2007). Predicting leaf physiology from simple plant and climate attributes: A global GLOPNET analysis. *Ecological Applications*, *17*, 1982–1988.

Reichstein, M., Falge, E., Baldocchi, D., Papale, D., Aubinet, M., Berbigier, P., … Grünwald, T. (2005). On the separation of net ecosystem exchange into assimilation and ecosystem respiration: Review and improved algorithm. *Global Change Biology*, *11*, 1424–1439.

Reu, B., Zaehle, S., Proulx, R., Bohn, K., Kleidon, A., Pavlick, R., & Schmidtlein, S. (2011). The role of plant functional trade-offs for biodiversity changes and biome shifts under scenarios of global climatic change. *Biogeosciences*, *8*, 1255–1266.

Santaren, D., Peylin, P., Bacour, C., Ciais, P., & Longdoz, B. (2014). Ecosystem model optimization using in situ flux observations: Benefit of Monte Carlo versus variational schemes and analyses of the year-to-year model performances. *Biogeosciences*, *11*, 7137–7158.

Santaren, D., Peylin, P., Viovy, N., & Ciais, P. (2007). Optimizing a process-based ecosystem model with eddy-covariance flux measurements: A pine forest in southern France. *Global Biogeochemical Cycles*, *21*, GB2013.

Schürmann, G., Kaminski, T., Köstler, C., Carvalhais, N., Voßbeck, M., Kattge, J., … Zaehle, S. (2016). Constraining a land-surface model with multiple observations by application of the MPI-Carbon Cycle Data Assimilation System V1.0. *Geoscientific Model Development*, *9*, 2999–3026.

Shi, Z., Sherry, R., Xu, X., Hararuk, O., Souza, L., Jiang, L., … Luo, Y. (2015). Evidence for long-term shift in plant community composition under decadal experimental warming. *Journal of Ecology*, *103*, 1131–1140.

Tarantola, A. (2005). *Inverse problem theory and methods for model parameter estimation*. Philadelphia, PA: Siam.

Thum, T., MacBean, N., Peylin, P., Bacour, C., Santaren, D., Longdoz, B., … Ciais, P. (2017). The potential benefit of using forest biomass data in addition to carbon and water flux measurements to constrain ecosystem model parameters: Case studies at two temperate forest sites. *Agricultural and Forest Meteorology*, *234–235*, 48–65.

Van de Weg, M. J., Meir, P., Grace, J., & Ramos, G. D. (2012). Photosynthetic parameters, dark respiration and leaf traits in the canopy of a Peruvian tropical montane cloud forest. *Oecologia*, *168*, 23–34.

Van Genuchten, M. T. (1980). A closed-form equation for predicting the hydraulic conductivity of unsaturated soils. *Soil Science Society of America Journal*, *44*, 892–898.

Van Ommen Kloeke, A., Douma, J., Ordonez, J., Reich, P., & Van Bodegom, P. (2012). Global quantification of contrasting leaf life span strategies for deciduous and evergreen species in response to environmental conditions. *Global Ecology and Biogeography*, *21*, 224–235.

Verheijen, L. M., Aerts, R., Brovkin, V., Cavender-Bares, J., Cornelissen, J. H. C., Kattge, J., & van Bodegom, P. M. (2015). Inclusion of ecologically based trait variation in plant functional types reduces the projected land carbon sink in an earth system model. *Global Change Biology*, *21*, 3074–3086.

Violle, C., Choler, P., Borgy, B., Garnier, E., Amiaud, B., Debarros, G., … Lavorel, S. (2015). Vegetation ecology meets ecosystem science: Permanent grasslands as a functional biogeography case study. *Science of the Total Environment*, *534*, 43–51.

Vuichard, N., & Papale, D. (2015). Filling the gaps in meteorological continuous data measured at FLUXNET sites with ERA-Interim reanalysis. *Earth System Science Data*, *7*, 157–171.

Wright, I. J., Reich, P. B., Cornelissen, J. H., Falster, D. S., Groom, P. K., Hikosaka, K., … Osada, N. (2005). Modulation of leaf economic traits and trait relationships by climate. *Global Ecology and Biogeography*, *14*, 411–421.

Wright, I. J., Reich, P. B., Westoby, M., Ackerly, D. D., Baruch, Z., Bongers, F., … Villar, R. (2004). The worldwide leaf economics spectrum. *Nature*, *428*, 821–827.

Wu, J., Jansson, P.-E., van der Linden, L., Pilegaard, K., Beier, C., & Ibrom, A. (2013). Modelling the decadal trend of ecosystem carbon fluxes demonstrates the important role of functional changes in a temperate deciduous forest. *Ecological Modelling*, *260*, 50–61.

Xia, J. Y., Luo, Y. Q., Wang, Y.-P., Weng, E. S., & Hararuk, O. (2012). A semi-analytical solution to accelerate spin-up of a coupled carbon and nitrogen land model to steady state. *Geoscientific Model Development*, *5*, 1259–1271.

Xu, X., Medvigy, D., Joseph Wright, S., Kitajima, K., Wu, J., Albert, L. P., … Pacala, S. W. (2017). Variations of leaf longevity in tropical moist forests predicted by a trait-driven carbon optimality model. *Ecology Letters*, *20*, 1097–1106.

BIOSKETCH

Marc Peaucelle did his PhD at the Climate and Environment Science Laboratory (LSCE, France). His research focuses on improving the representation of vegetation in the ORCHIDEE Dynamic Global Vegetation Model (DGVM). In particular, he is interested in improving the representation of plant functional types by a more continuous approach, exploring different ways to include the plasticity of plant functional traits.

SUPPORTING INFORMATION

Additional supporting information may be found online in the Supporting Information section at the end of the article.

How to cite this article: Peaucelle M, Bacour C, Ciais P, et al. Covariations between plant functional traits emerge from constraining parameterization of a terrestrial biosphere model. *Global Ecol Biogeogr.* 2019;28:1351–1365. https://doi.org/10.1111/geb.12937